Physics of the Earth and Planetary Interiors, 38 (1985) 92–109
Elsevier Science Publishers B.V., Amsterdam – Printed in The Netherlands

The near-source strong-motion accelerograms recorded by an experimental array in Tangshan, China

Kezhong Peng [1], Lili Xie [1], Shabai Li [1], D.M. Boore [2], W.D. Iwan [3] and T.L. Teng [4]

[1] *Institute of Engineering Mechanics, Academia Sinica (People's Republic of China)*
[2] *U.S. Geological Survey, Menlo Park, CA (U.S.A.)*
[3] *California Institute of Technology, Pasadena, CA (U.S.A.)*
[4] *University of Southern California, Los Angeles, CA (U.S.A.)*

(Received November 23, 1983; revision accepted August 16, 1984)

Peng, K., Xie, L., Li, S., Boore, D.M., Iwan, W.D. and Teng, T.L., 1985. The near-source strong-motion accelerograms recorded by an experimental array in Tangshan, China. Phys. Earth Planet. Inter., 38: 92–109.

A joint research project on strong-motion earthquake studies between the People's Republic of China and the United States is in progress. As a part of this project, an experimental strong-motion array, consisting of twelve Kinemetrics PDR-1 Digital Event Recorders, was deployed in the meizoseismal area of the $M_s = 7.8$ Tangshan earthquake of July 28, 1976. These instruments have automatic gain ranging, a specified dynamic range of 102 dB, a 2.5 s pre-event memory, programmable triggering, and are equipped with TCG-1B Time Code Generators with a stability of 3 parts in 10^7 over a range of 0–50°C. In 2 y of operation beginning July, 1982 a total of 603 near-source 3-component accelerograms were gathered from 243 earthquakes of magnitude $M_L = 1.2$–5.3. Most of these accelerograms have recorded the initial P-wave.

The configuration of the experimental array and a representative set of near-source strong-motion accelerograms are presented in this paper. The set of accelerograms exhibited were obtained during the $M_L = 5.3$ Lulong earthquake of October 19, 1982, when digital event recorders were triggered. The epicentral distances ranged from 4 to 41 km and the corresponding range of peak horizontal accelerations was $0.232g$ to $0.009g$. A preliminary analysis of the data indicates that compared to motions in the western United States, the peak acceleration attenuates much more rapidly in the Tangshan area. The scaling of peak acceleration with magnitude, however, is similar in the two regions. Data at more distant sites are needed to confirm the more rapid attenuation.

1. Description of array

A cooperative research project on strong-earthquake ground motion studies between the People's Republic of China and the United States of America started in 1981 (Boore et al., 1982) and is in progress now. The overall goal of this project is to increase the data base of strong ground motion of large earthquakes. Of particular interest are near-source data from great ($M \geq 8$) earthquakes, for which data are still lacking.

As a part of this project, an experimental strong-motion array was deployed in the meizoseismal area of the $M_s = 7.8$ Tangshan earthquake of July 28, 1976. Temporary installation of instruments in an area still experiencing aftershocks was expected to afford the opportunity to gain operational field experience with the system and also yield useful data.

The network was installed at an intersection of several active faulting structures (the Tangshan, Guye, Luanxian and Taoyuan fault structures) in the northeast part of the aftershock area of the Tangshan mainshock. Four digital accelerographs

0031-9201/85/$03.30

TABLE I

The condition of SMA stations on Tangshan array

Station identification				Site geology	Structure type/size	Instrument (PDR-1)		
No.	Name	Coord	Elevation (m)			S/N	Location	Installation
TS-01	Zhaogezhuang	39°45′39.7″(N) 118°24′18.9″(E)	76	Outcrop of basement rock of coal bed, depth of rock face $H_r = 0$ m	2-story-bldg.	117	Ground floor (cement)	Adhesive
TS-02	Beijiadian	39°44′29.2″(N) 118°28′31.6″(E)	40	Thickness of soil and sand is 12 m; Thickness of broken rock layer is 8 m; depth of rock face $H_r = 20$ m	1-story-bldg.	118	Cement floor	Adhesive
TS-03	Leizhuang	39°45′16.2″(N) 118°34′34.7″(E)	45	Thickness of soil layer, that consists of sand, clay, cobble and gravel, is about 50 m, $H_r = 50$ m	1-story-bldg.	116	Soil ground	Anchor
TS-04	Tuozitou (O.O.D.)	39°45′07.2″(N) 118°40′57.9″(E)	45	Thickness of sand layer is 52 m; Thickness of gravel is 18 m; depth of granite face $H_r = 70$ m	1-story-bldg.	115	Cement floor	Adhesive
TS-05	Tuozitou (B.A.)	39°45′02.4″(N) 118°40′55.8″(E)	45	Thickness of sand layer is 58 m; Thickness of gravel is 12 m; depth of granite face $H_r = 70$ m	1-story-bldg.	110	Cement floor	Adhesive
TS-06	Tuozitou (S.C.P.)	39°44′40.5″(N) 118°41′03.2″(E)	45	Thickness of soil layer is 48 m; Thickness of cobble is 12 m; depth of rock face $H_r = 60$ m	1-story-bldg.	111	Soil ground	Anchor
TS-07	Tuozitou (N.S.)	39°44′55.1″(N) 118°41′23.2″(E)	45	Thickness of soil layer, that consists of sand, clay, cobble and gravel, is 70 m, $H_r = 70$ m	1-story-bldg.	113	Cement floor	Adhesive
TS-08	Xiangtang	39°41′31.6″(N) 118°44′09.4″(E)	45	Outcrop of granite, on Taoyuan fault zone, $H_r = 0$ m	1-story-bldg.	108	Cement floor	Adhesive
TS-09	Luanxian	39°43′58.4″(N) 118°45′11.6″(E)	20	Soil layer consists of sand, clay, cobble and gravel, on fractured zone of Taoyuan fault.	1-story-bldg.	112	Soil ground	Anchor
TS-10	Shimen	39°43′47.0″(N) 118°50′47.4″(E)	30	Thickness of clay layer is 45 m, on eastern plate of Taoyuan fault, $H_r = 45$ m	1-story-bldg.	114	Cement floor	Adhesive
TS-11	Lulong (S.O.)	39°53′02.4″(N) 118°51′45.3″(E)	50	Thickness of sand and gravel is 3 m; depth of granite face $H_r = 3$ m; eastern plate of Taoyuan fault	4-story-bldg.	107	Ground floor (cement)	Adhesive
TS-12	Lulong (G.B.)	39°52′41.4″(N) 118°52′13.7″(E)	50	Thickness of sand and gravel is 10 m; on eastern plate of Taoyuan fault; depth of granite face $H_r = 10$ m	1-story-bldg.	109	Cement floor	Adhesive

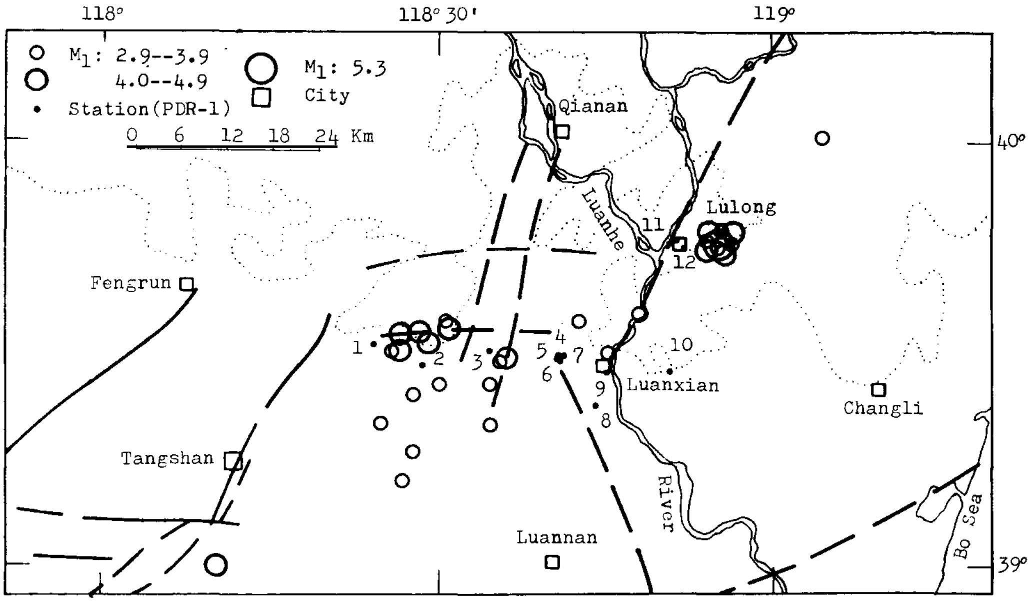

Fig. 1. Strong-motion accelerograph experimental array in Tangshan region and distribution of epicenters (1982.7–1983.3).
TS-01 Zhaogezhuang seismological station;
TS-02 Beijiadian refractory material factory;
TS-03 Leizhuang army office;
TS-04 Office of oil depot at Tuozitou;
TS-05 Business agency of oil depot at Tuozitou;
TS-06 Luanxian school of Communist Party at Tuozitou;
TS-07 Luanxian nurses' school at Tuozitou;
TS-08 Xiangtang seismological station;
TS-09 Luanxian seismological office;
TS-10 Shimen town office;
TS-11 Lulong seismological office;
TS-12 Lulong goods bureau.

were installed along the Luanxian and Taoyuan faults where moderate earthquake seismicity was high; eight digital accelerographs were sited along a line normal to the fault. Four of those eight instruments were concentrated in a small area of about 0.3 km^2, near the town of Tuozitou, to observe the variation of ground motion in a small area. Figure 1 shows the primary tectonic structures at the array site and the distribution of instruments. A brief description of the station sites is given in Table I.

2. Description of instrument used in array

The twelve digital accelerographs installed are Kinemetrics PDR-1 Digital Event Recorders, fitted with the FBA-13 Force Balance Accelerometer (Table II). A metal pinch roller was used to allow recording at cold temperatures.

To reduce the effects of buildings on the recorded ground motion, all the instruments were installed in small, light shelters (Fig. 2). For installation of instruments, the FBA-13 tri-axial accelerometer package was bolted to a steel plate which was then attached to the cement floor with either epoxy resin or anchor bars (Fig. 3). These methods of attachment are convenient and reliable.

The instruments are serviced at 10- to 43-day intervals. Problems associated with the effects of the cold winter temperatures on the batteries have been found in 57 out of 367 site visits. No mechanical problems due to the cold have been noted, although temperatures have dropped to $-20°C$.

TABLE II

Specifications of PDR-1/FBA-13

Number of channels	Three
Input filtering	Selectable 2.5, 12.5, 25, 50 Hz; 12 dB/oct roll-off
Gain-ranging	±36 dB up and down during event
Dynamic range	102 dB
Resolution	12-bit
Format	Phase-encoded 4-track; three data, one parity
Bit density	1280 bits/inch/track
Sample rate	100 or 200 samples s^{-1} per channel selectable
Tape speed	1.25 or 2.5in s^{-1}
Start-up time	150 ms
Trigger	STA/LTA selectable ratios or differences
Pre-event memory	Standard PEM is 2.56 s with 200 sps or 5 s with 100 sps
Temperature stability of TCG-1B	$\pm 3 \times 10^{-7}$ (0–50°C)
Full scale	$\pm 2g$
Natural frequency of FBA-13	50 Hz
Damping ratio of FBA-13	0.7
Power	+12 V and −12 V DC

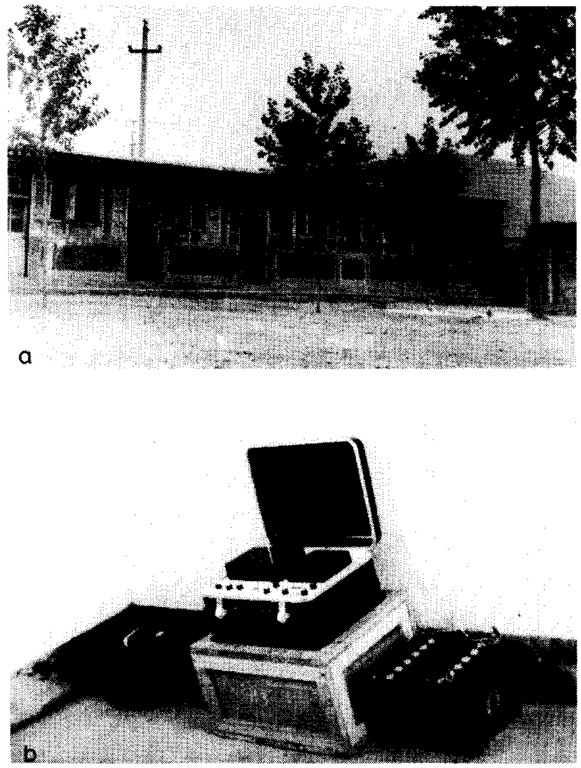

Fig. 2. (a) Exterior of a typical station (TS-10). (b) Installation of instruments (PDR-1/113 and FBA-13).

3. Near-source accelerograms

In the 9 months from July, 1982 to March, 1983, a total of 285 accelerograms have been obtained during 133 earthquakes of magnitude M_L from 1.2–5.3 (Table III). Two years of recordings have produced 603 records from 243 events (25 of

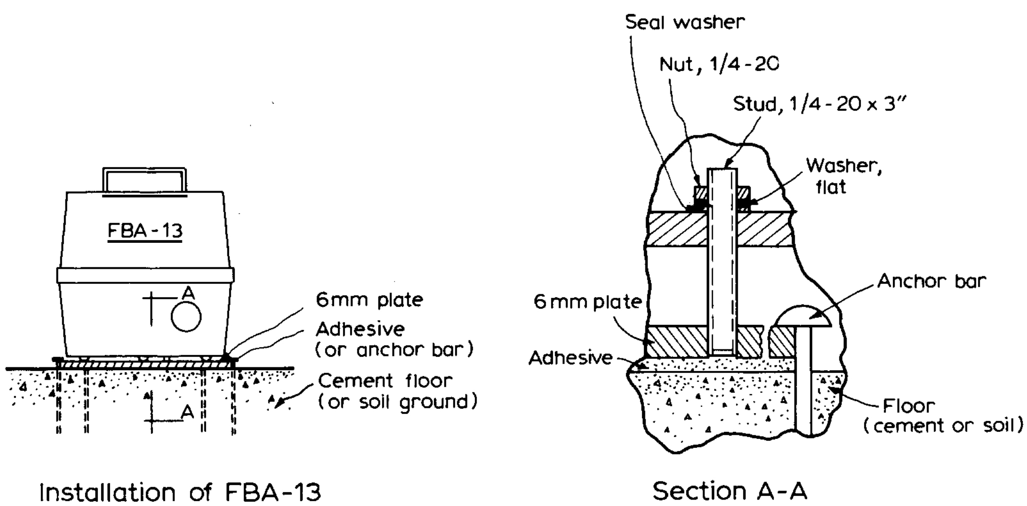

Fig. 3. Installation of FBA-13.

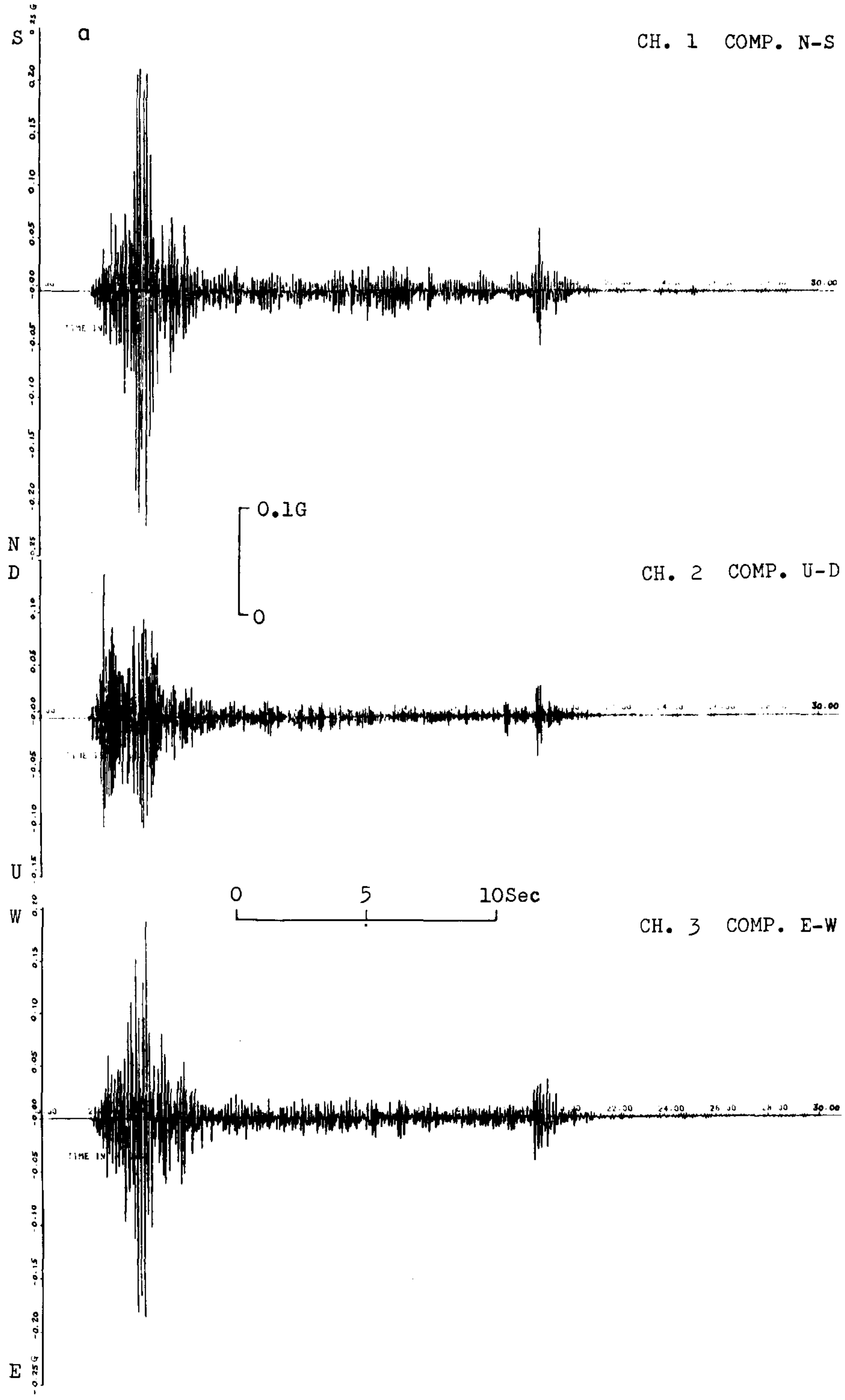

Fig. 4. Nine digital accelerographs tiggered during the Lulong earthquake. Event: 19/10/1982. 20:46′ (BJT), $M_l = 5.3$, Depth: 9.6 km, Lat. 39°52.6′ (N), Long. 118°55.4′(E). Station: Lulong City Goods Bureau (TS-12), Lat. 39°52′41″(N), Long. 118°52′14″(E). PDR-1/109 and FBA-13/16204,05,06 (Kinemetrics).

which had magnitudes > 4.0). Figure 1 shows the epicenters of some earthquakes ($M_L = 2.9$–5.3) during the period.

Nine digital accelerographs triggered during the Lulong earthquake of magnitude $M_L = 5.3$ of October 19, 1982 are shown in Fig. 4. The epi-

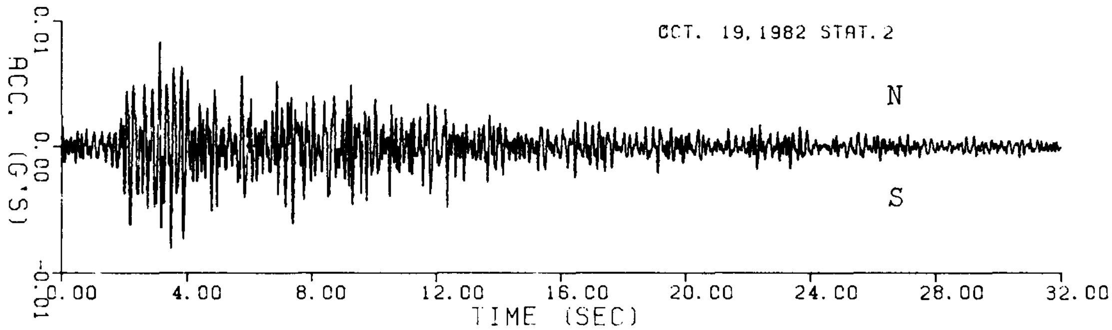

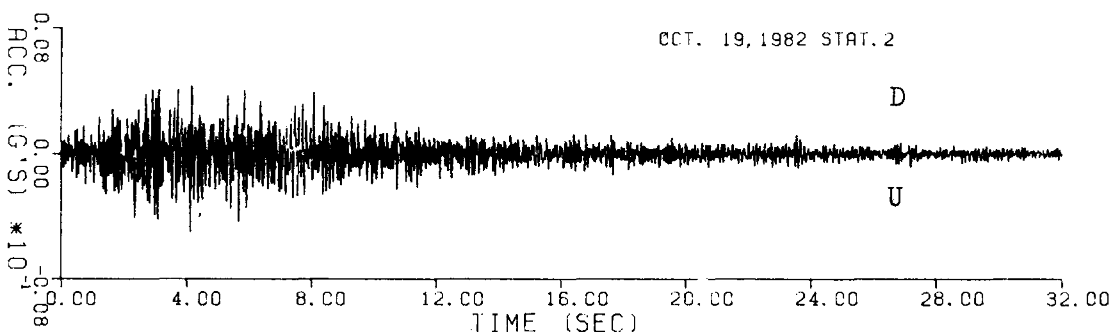

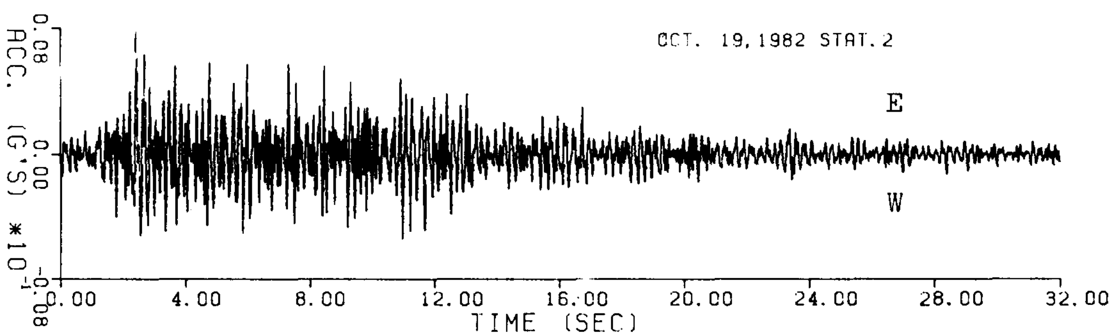

central distance of the nearest station (Lulong station, No. TS-12) is ~ 4.2 km; the farthest station is 40.5 km from the epicenter. The maximum peak horizontal acceleration of 0.232g and vertical acceleration of 0.128g were recorded at the nearest station. For this earthquake, the epicenter area is

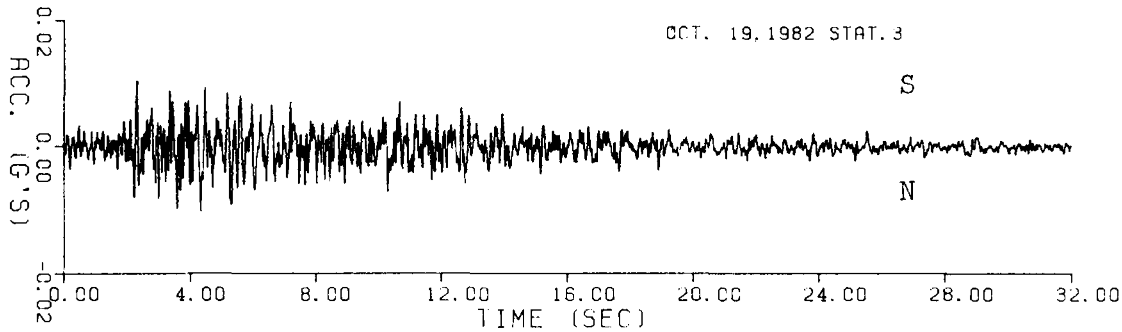

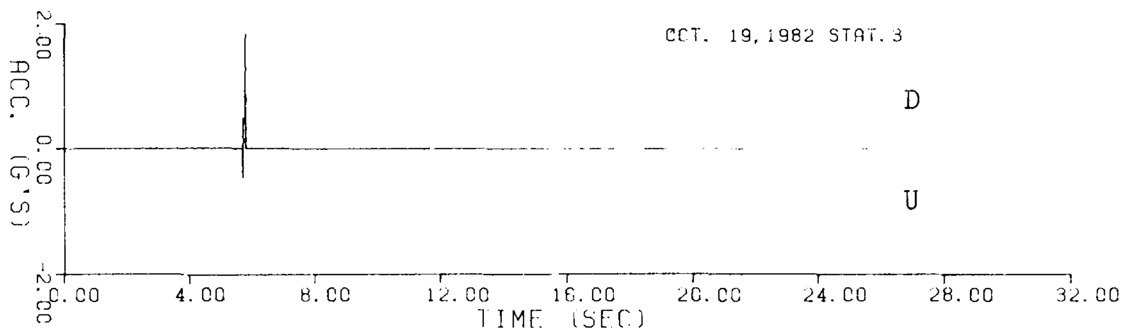

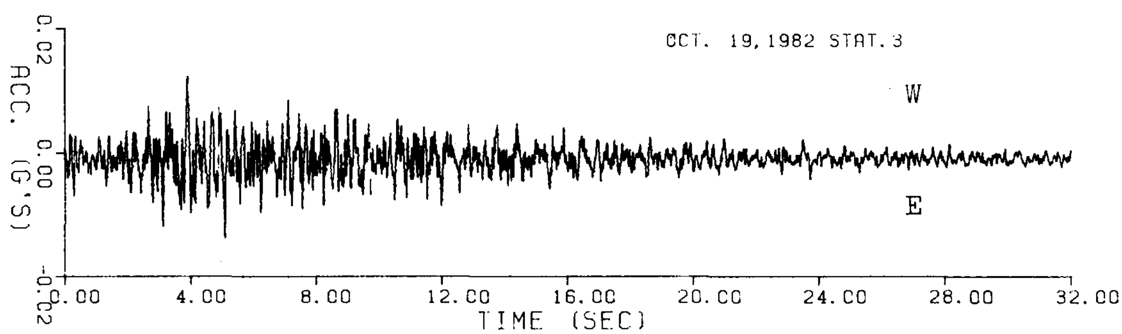

at Xiazhai Town where the rural masonry buildings suffered moderate damage.

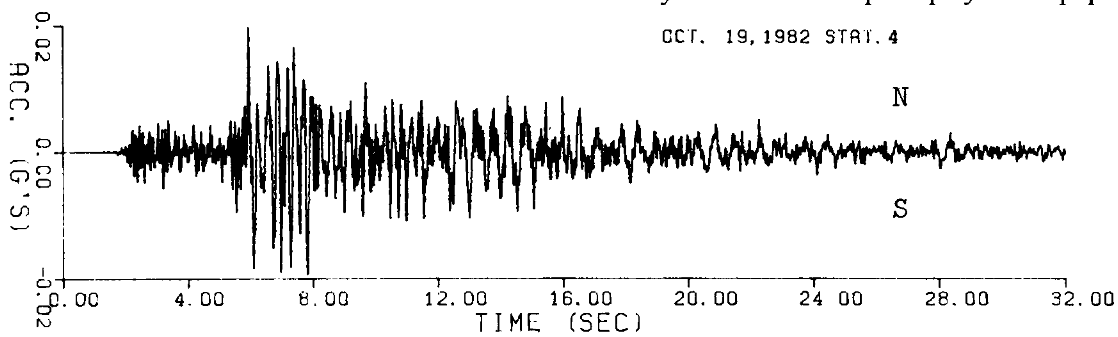

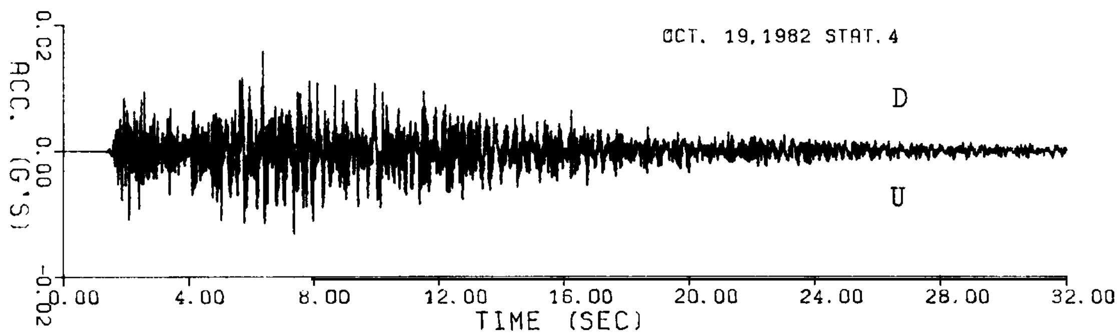

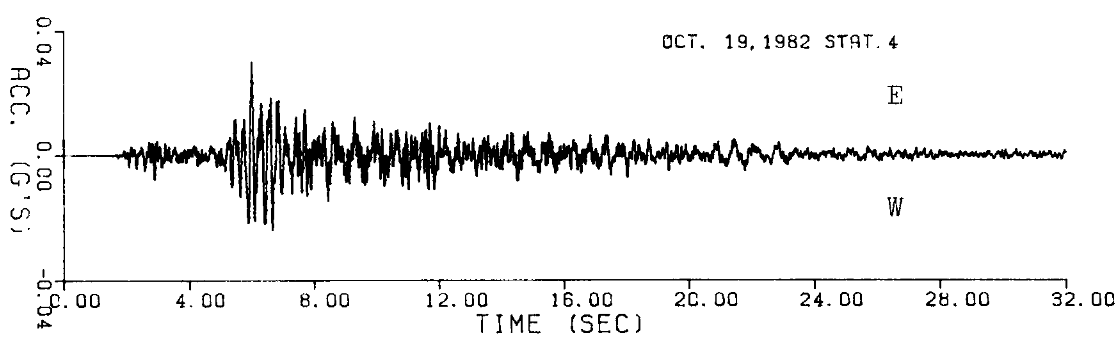

4. A preliminary analysis of analog accelerograms

A complete analysis of the data was hampered by the lack of adequate playback equipment. The necessary equipment has now been obtained, and a report describing the analysis will be published in the future. In this paper we provide several results obtained through a preliminary analysis of the visual playbacked records.

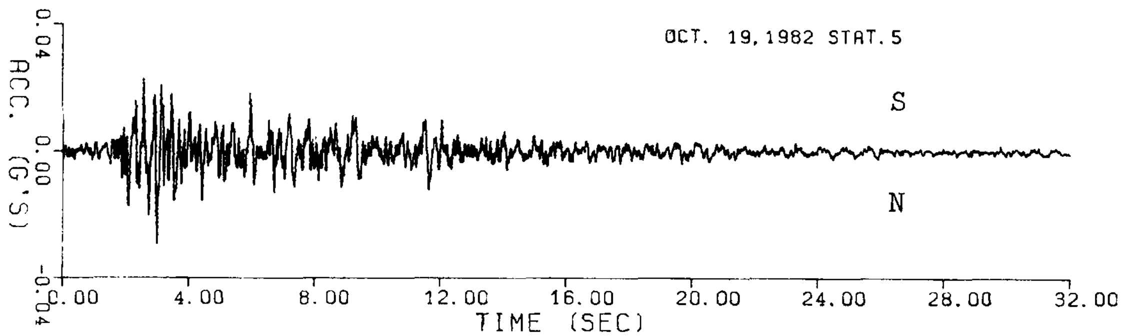

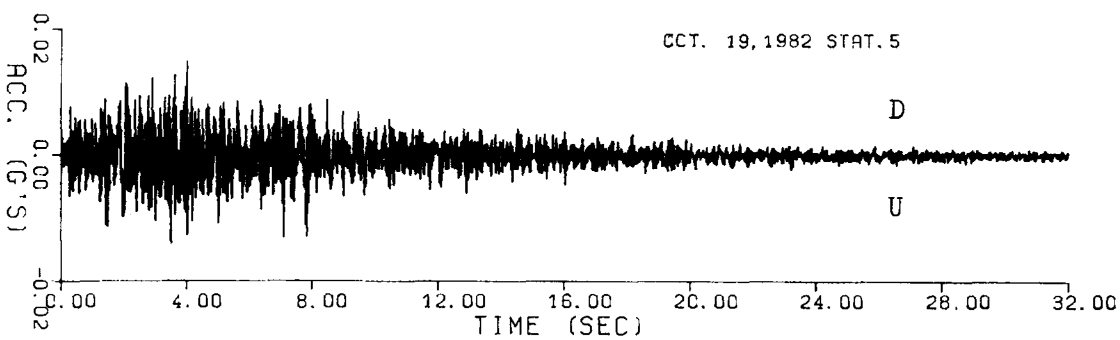

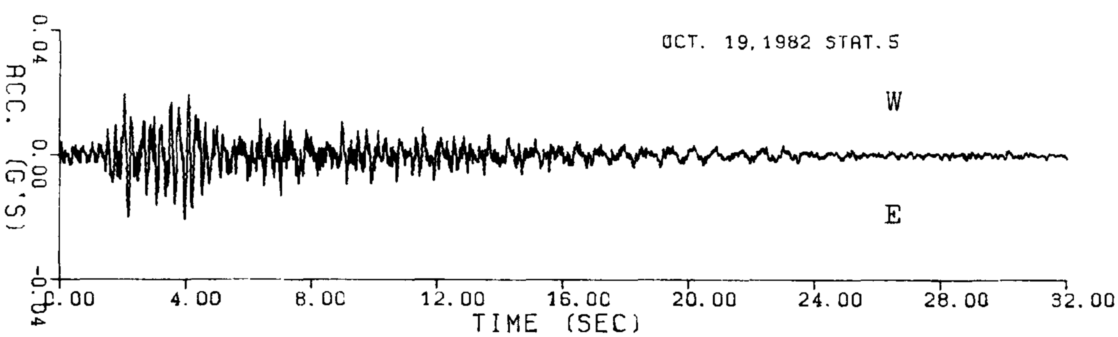

4.1. Determination of hypocenters

From absolute arrival times measured on the accelerograms, the origin times and source coordinates of the earthquakes have been determined by using the chord (Ishigawa) method. The locations are illustrated in Table IV and Fig. 5, and a comparison with the locations provided by the

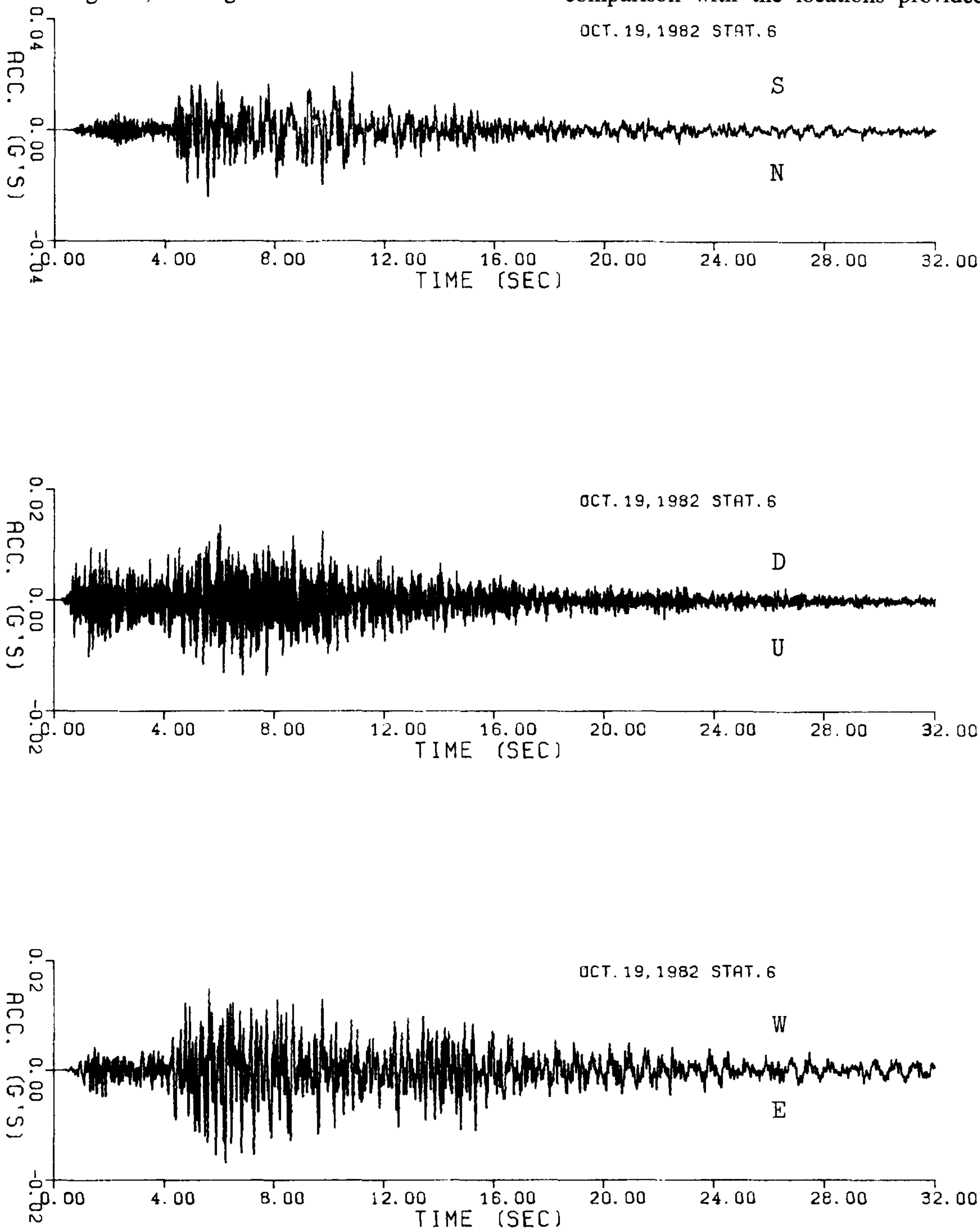

Institute of Geophysics (IGP), State Seismological Bureau of China (1977), using more distant data, is also given.

It is worth noting that the epicenter we located for the Lulong earthquake is much closer to the field investigated epicenter than is the IGP epi-

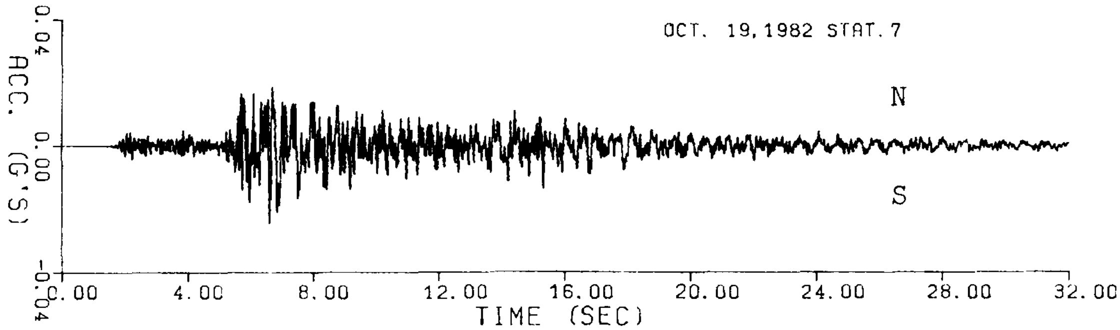

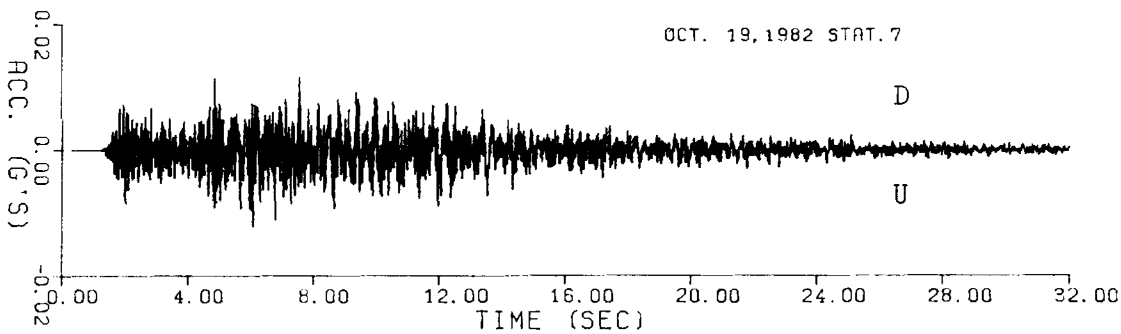

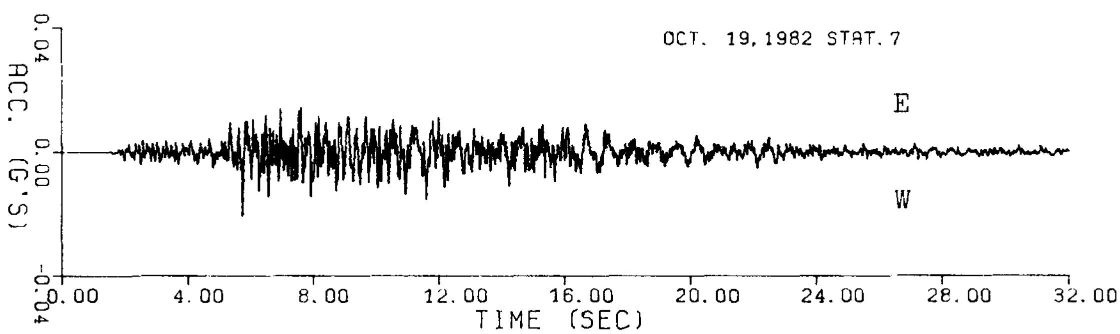

center. The improvement in the earthquake location obtained by using the strong-motion data emphasizes the utility of digital accelerographs; standard seismic stations close to large earthquakes are driven offscale and information about the arrival time of later seismic phases is lost.

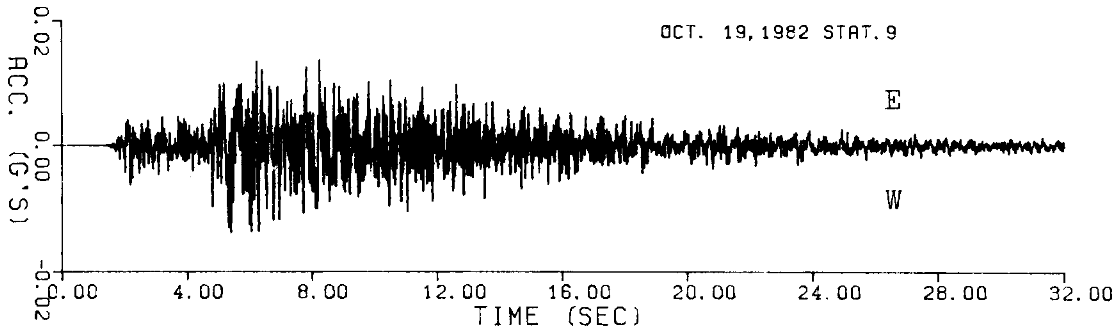

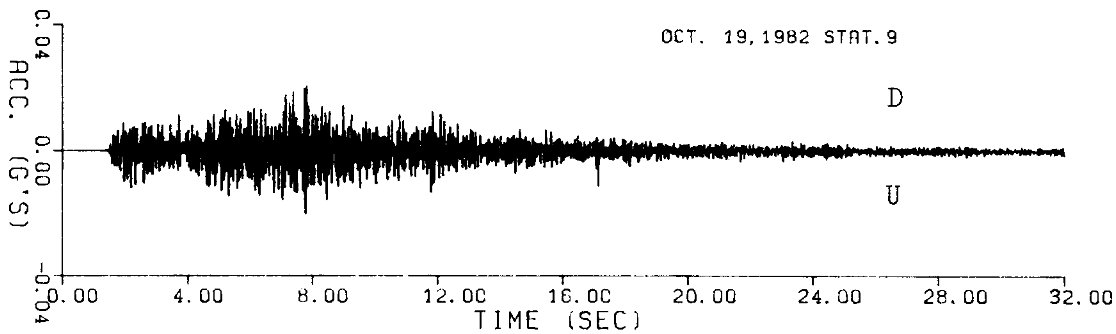

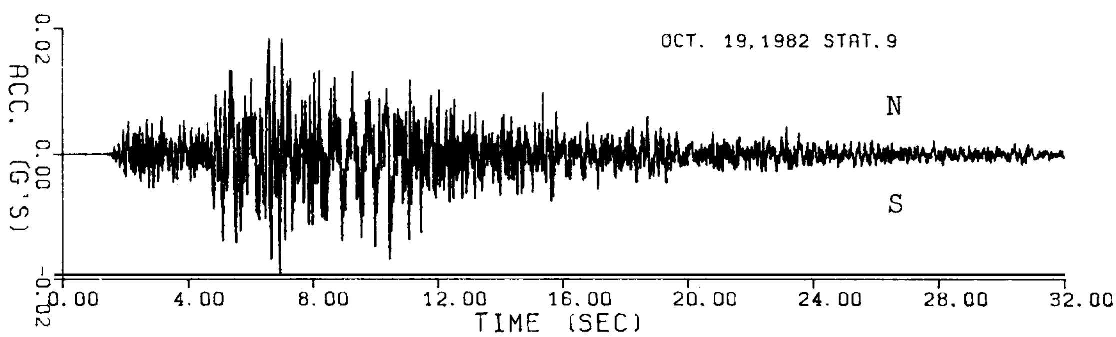

TABLE III

Number of Earthquake Records in Tangshan Array (1982.7–1983.3)

Magnitude M_l	1–1.9	2–2.9	3–3.9	4–4.9	5.3	Total
No. of events	3	102	16	11	1	133
No. of records	3	183	51	39	9	285

In addition to the hypocenter determination, the P- and S-wave velocities in the area are calculated as 5.58 km s^{-1} and 3.23 km s^{-1}, respectively, from P- and S-wave arrival times on the Lulong earthquake accelerograms (Table V).

4.2. The attenuation of peak ground acceleration A_m

A two-stage regression analysis (Joyner and Boore, 1981) has been used to fit the peak accelerations to the following regression model

$$A_m = \alpha \cdot 10^{(\beta M + \gamma R + \sigma)}/R \quad (1)$$

where

$$R = \sqrt{\Delta^2 + h^2}$$

and M is the local magnitude and Δ is the epicentral distance. α, β, γ, and h are regression parameters. σ is the standard deviation of the logarithm of a predicted value. Ninety-three measured horizontal accelerations (larger of two components) from 19 earthquakes ranging in magnitude from 2.9 to 5.3 were used in the regression analysis; for the vertical acceleration, 87 measurements from 19 events were used. Events recorded on only one station were excluded from the analysis.

The magnitudes used were provided by the Institute of Geophysics (IGP), as determined from the network of instruments in the Beijing-Tangshan area. The IGP uses Richter's correction for distance (Richter, 1958) and, for earthquakes with $M < 3.2$, the peak motion from once-integrated 1-Hz velocity transducers. For larger earthquakes, which saturate the 1-Hz instruments, measurements are made on seismograms obtained on a

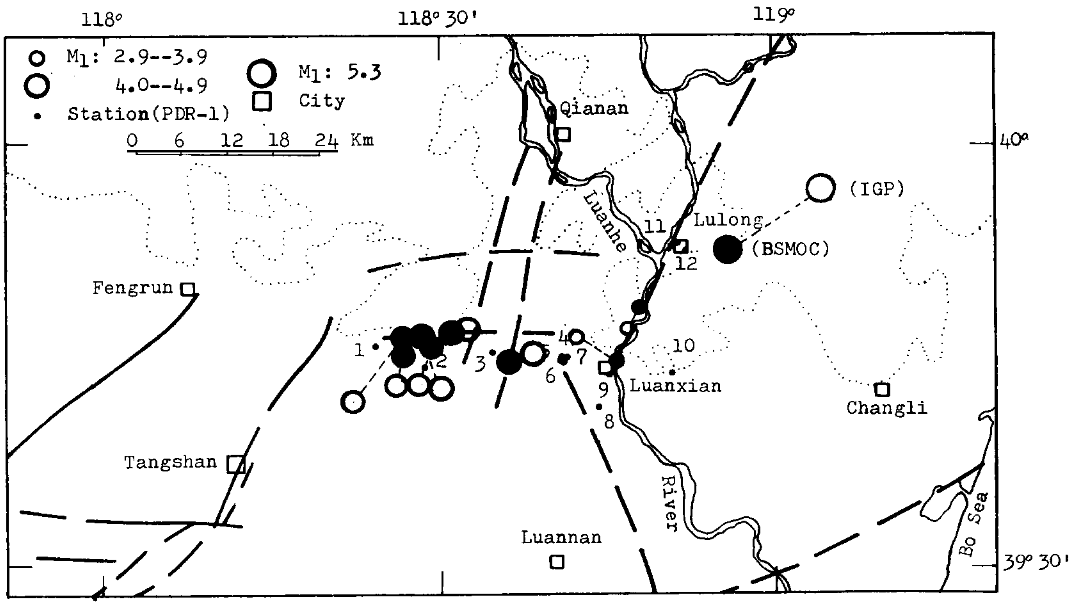

Fig. 5. Comparison of earthquake locations obtained from IGP and BSMOC/IEM.

TABLE IV

Comparison of earthquake parameters between IGP and BSMOC

Data source	Time of earthquake (Date, h:min's")	Location		Depth (km)	Magni. M_l
		Λ_E	Φ_N		
IGP	82.07.13,05:42'29.9"	118°42'	39°46'		2.9
BSMOC	05:42'30.0"	118°45.8'	39°44.7'	14.7	
IGP	82.07.17,12:42'55.9"	118°38'	39°45'		4.4
BSMOC	12:42'56.7"	118°36.0'	39°44.7'	8.4	
IGP	82.07.25,10:10'59.4"	118°47'	39°47'		3.1
BSMOC	10:10'59.3"	118°47.7'	39.48.4'	8.4	
IGP	82.10.19,20:45'59.2"	119°0.4'	39°57'		5.3 *
BSMOC	20:46'00.3"	118°55.4'	39°52.6'	9.6	
IGP	82.10.25,17:44'35.3"	118°26'	39°43'		4.3
BSMOC	17:44'35.5"	118°26.5'	39°44.9'	12.0	
IGP	82.11.21,01:01'36.5"	118°28'	39°43'		4.2
BSMOC	01:01'36.5"	118°28.8'	39°45.5'	12.9	
IGP	82.12.30,22:34'46.0"	118°22'	39°42'		4.4
BSMOC	22:34'46.5"	118°26.3'	39°45.9'	12.0	
IGP	83.03.04,04:03'20.5"	118°32'	39°47'		4.4
BSMOC	04:03'20.9"	118°31.3'	39°46.9'	7.7	
IGP	83.03.08,08:35'19.3"	118°30'	39°43'		4.0
BSMOC	08:35'19.3"	118°28.1'	39°46.4'	9.9	

Notes: * This value of magnitude is from Hebei Seismological Bureau. IGP–Institute of Geophysics/SSB. BSMOC–Beijing Strong Motion Observation Center/IEM.

lower-gain 12s instrument located in the basement of the IGP recording building (in these measurements, the longer period surface wave trains are ignored, even if they represent the peak motion). This recording site has a pronounced amplification factor, however, corresponding on the average to +0.5 magnitude units. Because this factor is still being studied, it is not applied to the magnitudes reported by the IGP (including those listed in the tables in this paper). For the regression analysis, however, reported magnitudes greater than 3.2 have been reduced by 0.5. Not doing so leads to a severe bias in the results. The only magnitude not corrected is that for the Lulong earthquake. The IGP reported $M = 6.2$; the value of 5.3 was obtained from a 12s instrument at another observation site in the Beijing area not used in routine analysis.

The analysis yielded the following empirical equations (Fig. 6a, b) for peak acceleration in g,

TABLE V

Data of V_p, V_s and V_φ from Lulong earthquake of Oct. 19th, 1982

No. of station	$\bar{p}$ travel-time (s)	$\bar{p}$ wave velocity (km s^{-1})	$\bar{s}$ travel-time (s)	$\bar{s}$ wave velocity (km s^{-1})
TS-04	5.070	5.550	8.710	3.231
TS-06	5.267	5.635	9.207	3.223
TS-07	4.868	5.620	8.408	3.254
TS-09	4.391	5.518	7.571	3.200
TS-10	3.805	5.566	6.585	3.216
Average		5.578		3.225
Standard deviation σ		0.049		0.020

Velocity of virtual wave $V_\varphi = 7.645$ (km s^{-1}).

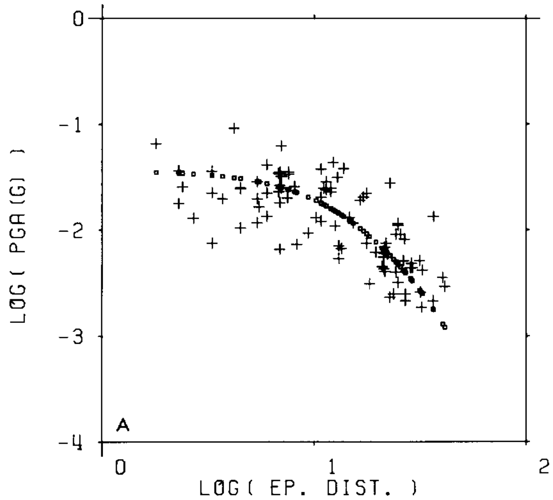

Fig. 6. (A) Data from events with more than 1 record horizontal data, reduced to $M = 4$.

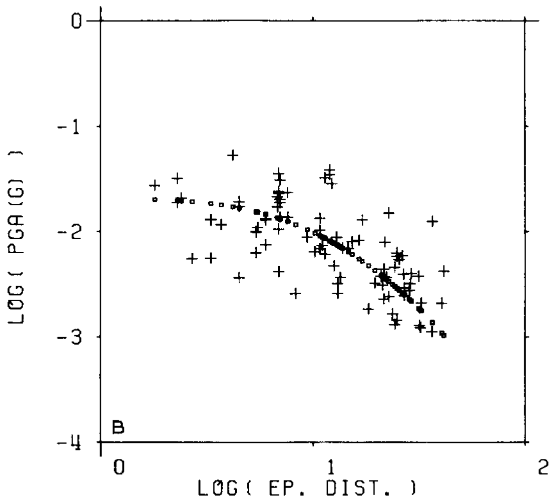

Fig. 6. (B) Data from events with more than 1 record vertical data, reduced to $M = 4$.

with distances in km

Horizontal: $\log A_m(H) =$

$$-1.49 + 0.31M - \log R - 0.0248R \pm 0.32 \quad (2a)$$

$$h = 9.4 \quad (2b)$$

Vertical: $\log A_m(V) =$

$$-1.92 + 0.29M - \log R - 0.0146R \pm 0.36 \quad (3a)$$

$$h = 6.7 \quad (3b)$$

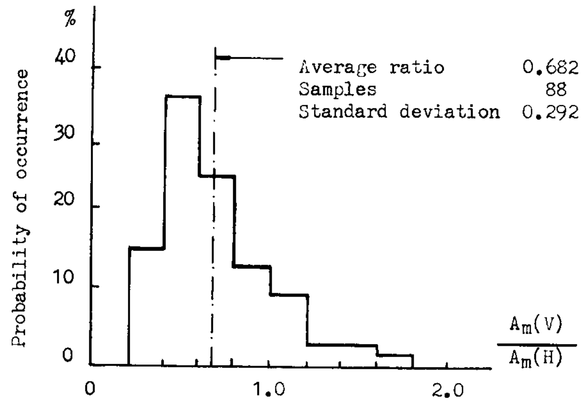

Fig. 7. Ratio between vertical and horizontal maximum acceleration.

These equations are preliminary; more refined equations await further studies of the magnitude and distances used in the analysis.

In an analysis of strong-motion data from earthquakes in western North America, Joyner et al. (1981) found

$\log A_m(H) =$

$$-1.97 + 0.41M_L - \log R - 0.0026R \pm 0.20 \quad (4a)$$

$$h = 9.2 \quad (4b)$$

for $6.4 \leq M_L \leq 7.2$. The magnitude scaling factor is higher than found from the Tangshan-area data, but the simulation model of Boore (1983) predicted that the magnitude scaling factor for large earthquakes should be ~ 0.1 units larger than for earthquakes with $3 < M_L < 5$. For this reason, the magnitude scaling factor found from the Tangshan-area data is in agreement with that found from western North American data (assuming that the magnitude M in eqns. 2 and 3 is equivalent to M_L). The attenuation factor, however, is ten times larger for the Tangshan region. Whether this attenuation factor is ruly representative of the actual attenuation in the region will require the analysis of data from greater distances and an investigation into possible biases introduced by the distribution of data in magnitude-distance space (as well as improved magnitude and distance estimates).

In Fig. 7, a distribution of the ratio $A_m(V)/A_m(H)$ of peak vertical acceleration to horizontal is shown and the mean ratio is 0.682 (88 data are used for statistical evaluation) and the standard deviation σ is 0.292.

4.3. The difference of ground motion in a small area

In the experimental array, 4 PDR-1 digital accelerographs (No. TS-04–TS-07) were installed at Tuozitou Town. The area surrounded by those four instruments is about 0.3 km^2. Although the ground here is flat, upon comparing the recorded peak accelerations at four stations, a distinct difference in both peak value of the same direction and orientation of ground motion recorded at each station is found for the same event. The biggest difference between peak accelerations in the same

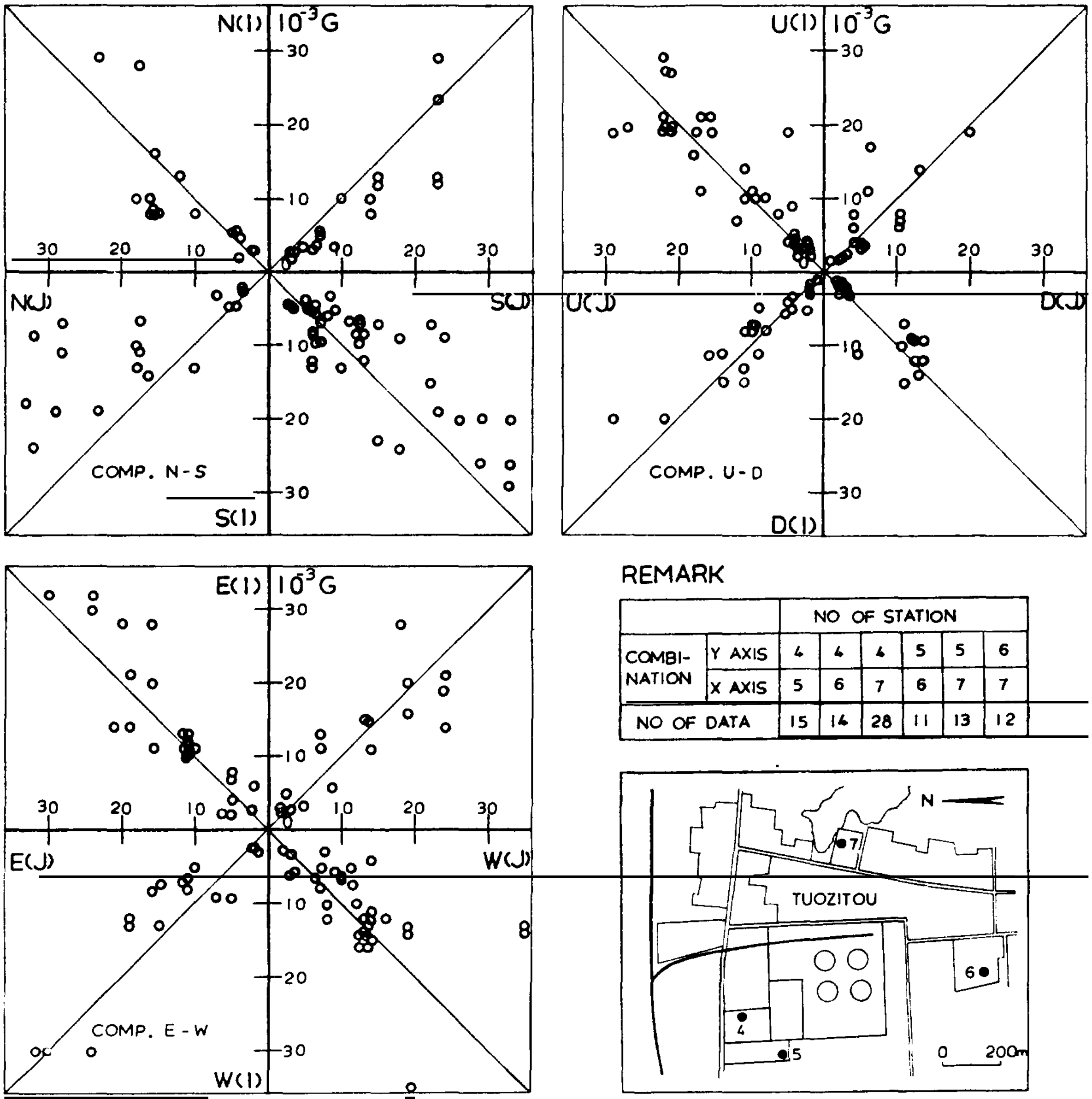

		NO OF STATION					
COMBI-NATION	Y AXIS	4	4	4	5	5	6
	X AXIS	5	6	7	6	7	7
NO OF DATA		15	14	28	11	13	12

Fig. 8. The difference of acceleration in a local area.

TABLE VI

Variation of peak ground acceleration over a small area

Time of events (Date, h-min-s)	Magnitude M_l	Average epicentral distance $\bar{\Delta}$ (km)	Component	Peak acceleration A_m (10^{-3} G)				Average peak acc. $\bar{A}_m$	Standard deviation σ (10^{-3} G)	$\sigma/\bar{A}_m$
				TS-04	TS-05	TS-06	TS-07			
1982.07.17			N–S	20.0	26.0	29.0	33.0	27.0	5.5	0.203
12-42-56.7	4.4	7.1	U–D	19.0	20.0	29.0	22.0	22.5	4.5	0.200
			E–W	30.0	32.0	30.0	24.0	29.0	3.5	0.119
1982.07.17			N–S	13.0	10.0	10.0	18.0	12.8	3.8	0.296
12-43-19.2	3.7	7.1	U–D	8.0	10.0	11.0	8.0	9.3	1.5	0.162
			E–W	14.0	13.0	35.0	19.0	20.3	10.2	0.503
1982.07.25			N–S	13.0	12.0	22.8	15.0	15.7	4.9	0.312
10-10-59.3	3.1	11.9	U–D	19.0	21.0	15.6	17.7	18.3	2.3	0.124
			E–W	13.0	6.6	11.6	11.0	10.6	2.8	0.262
1982.08.09			N–S	9.6	7.1	6.5	12.5	8.9	2.7	0.306
01-23-41.7	2.3	2.0	U–D	4.8	9.0	5.4	4.4	5.9	2.1	0.357
			E–W	7.9	11.2	6.9	14.7	10.2	3.5	0.347
1982.08.31			N–S	8.8	24.0	18.0	32.0	20.7	9.8	0.473
19-58-40.9	2.5	7.7	U–D	8.8	12.0	13.7	12.5	11.8	2.1	0.178
			E–W	14.4	16.0	12.4	13.5	14.1	1.5	0.108
1982.09.14			N–S	8.1	10.0	13.7	16.3	12.0	3.7	0.306
12-42-09.9	2.4	8.4	U–D	7.0	10.0	10.6	9.4	9.3	1.6	0.171
			E–W	13.8	21.0	19.0	23.8	19.4	4.2	0.218
1982.10.19			N–S	19.0	29.0	23.0	23.0	23.5	4.1	0.175
20-46-00.3	5.3	24.9	U–D	15.0	14.0	13.0	11.0	13.3	1.7	0.129
			E–W	28.0	20.0	16.0	19.0	20.8	5.1	0.247
1982.11.30			N–S	8.5	12.0	13.0	6.0	9.9	3.2	0.326
22-53-48.4	2.7	14.4	U–D	7.8	6.3	10.5	4.1	7.2	2.7	0.375
			E–W	11.0	10.2	11.5	11.0	10.9	0.5	0.049

direction at four stations is sometimes as great as 200–300% (Fig. 8). To illustrate this phenomenon, a scheme for such comparison is shown in Fig. 8. In 8a, b, the x and y coordinates, respectively, represent the peak horizontal acceleration in the same direction for the same earthquake recorded at any two different stations. Figure 8c shows the same relation for the peak vertical accelerations. The spatial variation in peak motions is given by the scatter of the points about the two straight lines with slopes of ± 1.

Additionally, there are eight earthquakes during which all the four stations obtained the records. The mean value A_m and a standard deviation σ of those peak accelerations and the ratio σ/A_m are listed in Table VI. The results verify that considerable differences can exist in peak ground accelerations in a small area. For this reason, it seems reasonable to consider the mean of peak accelerations at several points in a small area as a measure of the intensity of strong ground motion.

Acknowledgments

The writers wish to acknowledge the support of the State Seismological Bureau of China and U.S. National Science Foundation. The writers also wish to express their deepest thanks to An Yanru, Ding Feng, Du Meiqi, Du Ming, Ren Zhengyun, Wang Tiehua, Wu Weilian, Yan Jianwu, Yu Shuangjiu, Yu Shuqin and Zhao Shufang for their contributions of operating the Tangshan Experimental Strong-Motion Array and processing the data. Information regarding magnitude determination was obtained through discussions with Professor Qin Xinling and Mr. Fu Yu of the Institute of Geophysics. Art McGarr of the U.S.G.S. provided a critical review of the paper.

References

Boore, D.M., 1983. Stochastic simulation of high-frequency ground motions based on seismological models of the radiated spectra. Bull. Seismol. Soc. Am., 73: 1865–1894.

Boore, D.M., Hsieh, L.L., Iwan, W.D., Peng, K.Z. and Teng, T.L., 1982. U.S.A.–P.R.C. cooperative project on strong ground motion. Proceedings of U.S.–P.R.C. Bilateral Workshop on Earthquake Engineering, vol. 1, A 1, Harbin, China.

Institute of Geophysics of State Seismological Bureau, 1977. Analysis of Near-Earthquake. Earthquake Press, Beijing. (in Chinese).

Joyner, W.B. and Boore, D.M., 1981. Peak horizontal acceleration and velocity from strong-motion records including records from the 1979 Imperial Valley, California, earthquake. Bull. Seismol. Soc. Am., 71: 2011–2038.

Joyner, W.B., Boore, D.M. and Porcella, R.L., 1981. Peak horizontal acceleration and velocity from strong-motion records. Earthquake Notes, 52: 80–81 (Abstract).

Richter, C.F., 1958. Elementary Seismology. W.H. Freeman and Co., San Francisco, Chap. 22: 338–343.